

We are IntechOpen, the world's leading publisher of Open Access books Built by scientists, for scientists

6,900

Open access books available

185,000

International authors and editors

200M

Downloads

Our authors are among the

154

Countries delivered to

TOP 1%

most cited scientists

12.2%

Contributors from top 500 universities



WEB OF SCIENCE™

Selection of our books indexed in the Book Citation Index
in Web of Science™ Core Collection (BKCI)

Interested in publishing with us?
Contact book.department@intechopen.com

Numbers displayed above are based on latest data collected.
For more information visit www.intechopen.com



Sorption Capacities of a Lignin-Based Electrospun Nanofibrous Material for Pharmaceutical Residues Remediation in Water

Alexandre Camiré, Bruno Chabot and André Lajeunesse

Abstract

The threat of pharmaceutical residues in natural waters is a pressing concern in both developed and underdeveloped countries. Originating mostly from municipal and farms effluents, pharmaceuticals, poorly eliminated by traditional wastewater treatments enter the environment through sewage treatment plants discharges. Their adsorption on ecological adsorptive materials such as lignin may represent an interesting remediation solution. The present study sets out the sorption capacities and properties of a newly developed lignin-based nanofibrous material for typical pharmaceutical residues (fluoxetine, venlafaxine, ibuprofen, and carbamazepine) found in surface waters. This green biomaterial showed, in addition to its high recovery yield, excellent reusability through desorption (more than 90% recovered). As an example, adsorption levels reached 78 mg/g for adsorption of fluoxetine compared to 5–10, 49 and 75–80 for unfunctionalized silica, zeolites and ion-exchange resins respectively. The innovative approach reported therein perfectly meets the concept of circular economy sought in modern societies.

Keywords: adsorption-desorption cycles, electrospinning, lignin, pharmaceutical residues, kinetics, isotherms, wastewater

1. Introduction

As water scarcity becomes even more present in underdeveloped countries, developed states have to face a different challenge: water pollution from emerging contaminants [1]. Pollutants such as pharmaceutical residues come in a variety of forms and origins causing great issues [2, 3]. Many measures are established to reduce such contamination mostly in the form of water treatments and legislation [1]. However, great limitations are associated with the traditional techniques used in wastewater treatment plants. Most of them are due to either their cost or their low removal efficiency on emerging contaminants [4, 5]. For instance, degradation processes such as ozonation or chlorination were proven efficient for the degradation of organic molecules [6, 7]. However, these techniques have high operational costs and often cause dangerous degradation by-products that would follow the water flow and end up in rivers and lakes [8].

A specific technique distinguishes itself from the others; sorption. Such a treatment has the advantage of capturing contaminants with lower operational costs and without generating any dangerous by-products [5]. The most exploited sorbent is activated carbon (AC) which has high adsorption capacity and low specificity [5, 9]. Its efficiency comes from its high surface area on which contaminants can be adsorbed through interaction forces such as van der Waals [5]. It is often used for water purification through commercially available filters. Activated carbon can be made from various biological residues giving value to waste [9–11]. However, the synthesis of ACs necessitates the carbonization of the material itself and an activation step which can be costly and not environmentally friendly [5].

Another option is the production of adsorbents from highly available natural polymers. Therefore, the product would be green, inexpensive and biocompatible. As many biosorbents are still being studied throughout the world, their potential is not fully exploited, and low attention is given to polymers such as lignin. Lignin, the second most abundant biopolymer after cellulose, is a naturally occurring polymer composing wood at 20–40% [12, 13]. Giving resistance and rigidity to the cell walls of plants, this biopolymer is water insoluble and resistant to organic solvents [12]. Lignin is also a highly variable biopolymer which is composed of its three main monomers (coniferyl alcohol, sinapyl alcohol and p-coumaryl alcohol) in a random pattern [13]. Its composition is further randomized by the addition of functional groups (mainly sulfate and carboxyl groups) during its extraction phase [13]. Even though it is variable, all lignins contain phenols, aliphatic alcohols and ethers [14]. Right now, lignin is mostly used to produce energy in the pulp and paper industry (where it is mainly extracted) and regenerate chemical reagents [15]. Although it is not its main use, lignin has already been used as an adsorbent for heavy metals or even dyes [16–19]. However, to our best knowledge, lignin has never been tested for pharmaceutical residues removal at trace levels. Therefore, the development of this lignin-based electrospun nanofibrous materials open up new opportunities for reducing inputs of pharmaceuticals into the environment.

To be able to achieve a satisfying adsorption capacity for trace contaminants and compete with AC, it is necessary to increase the surface area of the material. A simple way is the transformation of the polymer into nanofibres through electrospinning. This technique exploits the stretching of polymers exposed to a high voltage under defined experimental conditions [20, 21]. In electrospinning, a polymer is dissolved and introduced into a syringe (see **Figure 1**). Voltage is applied between the needle of the syringe and a collector plate. As a drop is formed at the tip of the needle, its surface tension will be disrupted by the electrical field and cause a Taylor cone and the formation of the fibres [22, 23]. Typically, fibres as thin as the nanometres scale are obtainable through this method [20, 24]. Because of its

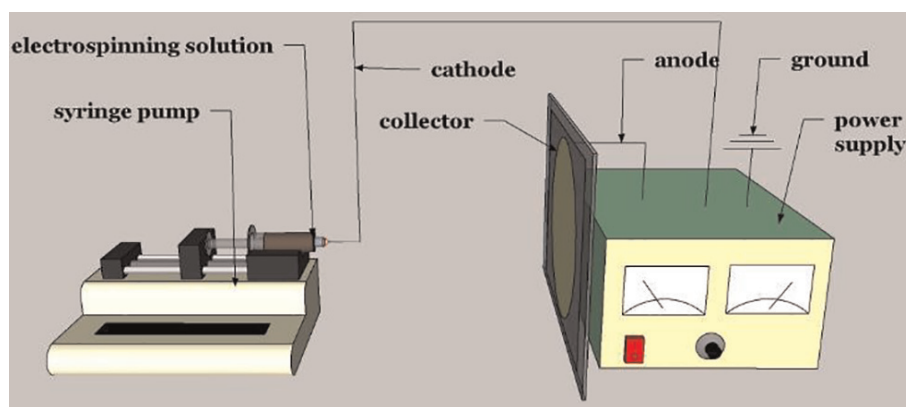


Figure 1.
Typical electrospinning setup.

limited known uses, the electrospinning of lignin is not popular even if its electrospinnability with a co-polymer is known [23–25]. Hence, the material and the application are unprecedented.

In this study, electrospun lignin nanofibres will be exploited for the adsorption of pharmaceutical residues in water. Precisely, fluoxetine and venlafaxine (antidepressant), carbamazepine (anticonvulsant) and ibuprofen (anti-inflammatory) will be tested for adsorption on developed nanofibres. The material's adsorption will be characterized by kinetic and isotherm studies. Its capacity to be reusable will also be determined by using various desorption environments.

2. Methodology

2.1 Chemicals and equipment

Alkali lignin (AL) low sulfur (28,000 Da, CAS 8064-05-1) and poly (vinyl alcohol) (PVA) 98–99% hydrolysis (31,000–50,000 Da, CAS 9002-89-5) were provided by Sigma-Aldrich (St-Louis, MO, USA). Sodium hydroxide pellets (NaOH) 98% (CAS 1310-73-2) and methanol HPLC grade (CAS-67-51-1) were provided by Alfa Aesar (Ward Hill, MA, USA). Hydrochloric acid (CAS 7647-01-0), acetonitrile HPLC grade (CAS 75-05-8), sodium citrate dihydrate (CAS 6132-04-3), sodium chloride (CAS 7647-14-5) and o-phosphoric acid HPLC grade 85% v/v (CAS 7664-38-2) were purchased from Fisher Scientific (Fair Lawn, NJ, USA). Fluoxetine hydrochloride (FLX) (CAS 56296-78-7), venlafaxine hydrochloride (VEN) (CAS 99300-78-4), carbamazepine (CAR) (CAS 298-46-4) and ibuprofen (IBU) (CAS 15687-27-1) were provided by Sigma-Aldrich (Oakville, ON, Canada). Citric acid anhydrous (CAS 77-92-9) was provided by Jungbunzlauer (Bale, Swiss). Commercial adsorbents used for comparison were Amberlyst[®] 15 (CAS 39389-20-3), Dowex[®] Marathon[®] C (CAS 69011-20-7), SiliaFlash[®] F60 40–60 µm particle size, fumed silica (CAS 112945-52-5) and Valfor[®] 100 sodium aluminosilicate zeolite respectively from Alfa Aesar (Ward Hill, MA, USA), Sigma-Aldrich (St-Louis, MO, USA), Silicycle (Quebec City, QC, Canada), and The PQ Corporation (Valley Forge, PA, USA).

The electrospinning setup was composed of a syringe pump (Kd scientific) and a power supply (Gamma High Voltage Research). Two laboratory ovens (Fisher Scientific Isotemp Oven and ThermoScientific HERATharm oven) were used for conservation and stabilization of the membranes. An orbital shaker (Lab Line model 3520) and an environmental orbital shaker incubator (Lab Line model 3528) were used for adsorption tests. Nanofibres were characterized using a Hitachi SUI510 scanning electron microscope (SEM). A Shimadzu Prominence I-series high performance liquid chromatograph (HPLC) coupled with a diode array detector (DAD) with a reverse phase column XB-C18, 100 Å, 150 × 3 mm, 2.6 µm particle size (Phenomenex, Kinetex[®]) was used to analyze contaminated water samples.

2.2 Electrospinning solution preparation

The electrospinning solutions were prepared as reported in Camire et al. [26]. Briefly, solution of AL and PVA 15% wt were prepared by dissolving AL in NaOH 1 M and PVA in water heated to 80°C for 60 min. After the dissolution, both solutions were mixed in a mass ratio of 1:1. This solution was stirred for an hour and settled at room temperature for another hour. The AL:PVA solution was then used directly for electrospinning or kept at 4°C in a refrigerator for a maximum of

1 month. Before use, the refrigerated solution was brought to room temperature in a hot water bath for an hour.

2.3 Electrospinning

The previous prepared solution was injected in a 5 mL syringe with a 20-gauge needle for electrospinning. The syringe was set to the syringe pump and voltage was applied between the needle and the collector. The collector was a non-stick cookie sheet giving good electrospinning, reusability and easy recovery of the nanofibres. The electrospinning parameters were based on results obtained previously [26]. The conditions were a flow rate of 0.1 mL/h with an applied DC voltage of 15 kV. The collector was placed 20 cm away from the tip of the needle. The temperature was kept at 22°C and relative humidity maintained between 10 and 40%. A razor blade was used to recover the nanofibrous mat from the collector. All experiments were conducted in a customized electrospinning box. The electrospun nanofibre mat was then kept overnight in a laboratory oven at 80°C for drying and stabilization purposes.

2.4 Nanofibre stabilization

Due to electrospun nanofibres' high solubility in water, AL:PVA nanofibres mats were stabilized using two consecutive techniques. Both techniques are based on previous works [26]. The first method used the glass transition temperature of polymers to raise their crystallinity and hence their water resistance. Therefore, nanofibres were heated in a laboratory oven at 160°C for 3 h. Next, the membranes were immersed in a 0.5 M sodium citrate buffer pH 4.5 for a period of 3 h. This process aims to protonate AL's phenol groups which were previously deprotonated during the preparation of the electrospinning solution in a method similar to the extraction methods of black liquor [15]. During this step, the morphology of the membrane changes drastically due to the dissolution of a part of the PVA. The dissolution causes a rise in the concentration of AL (the membranes become browner) and cross-linking of the nanofibres. After exposure to the buffer, the membranes were washed several times with purified water, stretched and dried on a metallic surface. Finally, the nanofibrous mats were recovered using a razor blade.

2.5 Adsorption tests

In this section, three types of tests were performed: adsorption of a single contaminant on AL:PVA membranes as well as commercial adsorbents, and adsorption of multiple contaminants on AL:PVA membranes. All adsorption tests were conducted in batches by adding a defined amount of adsorbent to a stirred solution containing a specific concentration of contaminants. All tested solutions were composed of purified water with 5% of methanol and contaminants adjusted at the targeted concentration. The organic solvent's purpose was to ensure that pharmaceuticals were solubilized in water. Separate 2500 ppm standard solutions of FLX, VEN, CAR and IBU were prepared by dissolving the corresponding stock solutions in methanol. Those solutions were then diluted for adsorption tests. Before, during and after the adsorption test, aliquots of 500 µL of the contaminated water were sampled, diluted with 500 µL of mobile phase, vortexed and injected in HPLC-DAD to determine the concentration of contaminants in solution. For tests using one contaminant on AL:PVA membranes, 50 ppm FLX solution was used as a model contaminated water. For tests with commercial adsorbents, adjustments were made to compensate for the size difference between adsorbents. Therefore, solutions of 250 ppm FLX in 10 mL were prepared to keep the same contaminant to

adsorbent mass ratio. For tests with multiple contaminants, 12.5 ppm of FLX, IBU, CAR and VEN were added to water to simulate contaminated water.

The adsorption tests were initialized by the addition of 25 mg of adsorbent (nanofibres or commercial adsorbent) to the solution. The tests were conducted over a period of 150 min to ensure that equilibrium was reached. Using a calibration curve and the area under the peaks on the chromatograms, the remaining concentration of the solution was calculated. From this value, the adsorption capacity at time t (Q_t) was calculated using the following equation:

$$Q_t = \frac{(C_0 - C_t)}{m} \times V \quad (1)$$

where C_t is the concentration of the contaminant (ppm) at time t (min), C_0 is the initial concentration of contaminants (ppm), V is the volume of the solution (L), and m is the mass of adsorbents (g).

For samples containing one contaminant, samples injected in HPLC-DAD were eluted using a mobile phase composed of acetonitrile and a 0.1% solution of phosphoric acid (60:40% v/v ratio). The flow rate was adjusted at 0.45 mL/min for 3.75 min with a detection at 230 nm. For samples containing more than one contaminant, the mobile phase was composed of acetonitrile and 0.1% phosphoric acid with a ratio of 40:60% v/v. The flow rate was adjusted to 0.5 mL/min for a period of 20 min with a detection still at 230 nm. In all cases, 10 μ L of the samples were injected using an autosampler. For all contaminants, a 10-point (0.5–100 ppm) calibration curve was established to determine the concentration. All tests were performed in triplicate.

2.6 Kinetic studies

Kinetic curves were obtained by sampling at intervals during the adsorption process. Samples were collected at 0, 5, 10, 15, 20, 30, 40, 50, 60, 75, 90, 120 and 150 min after the addition of the adsorbent. The equilibrium time of 150 min was determined by an initial kinetic test. The same sampling and injection processes as traditional adsorption tests were conducted for kinetic studies. By calculating the adsorption capacity through time, it is possible to obtain a kinetic curve which can be compared to adsorption kinetic models. Adsorption kinetic models give crucial information on the adsorption parameters and the limiting processes occurring during the adsorption. Typically, three steps occur during the adsorption: transfer of the adsorbate to the external surface of the adsorbent, internal diffusion of the adsorbate to active sites and sorption reaction with the adsorbent [27, 28]. In this study, three models were compared: pseudo-first order, pseudo-second order and Elovich. In all cases, the kinetic constants were calculated using Matlab's curve fitting app. To determine the best fitting model, determination coefficients and root of mean square errors (RMSE) were compared. The pseudo-first order model is represented by Eq. (2):

$$Q_t = Q_e(1 - e^{-k_1 t}) \quad (2)$$

In Eq. (2), Q_e corresponds to the adsorption capacity at equilibrium (mg/g), Q_t the adsorption capacity (mg/g) at time t (min) and k_1 the pseudo-first order kinetic adsorption constant (min^{-1}) [10, 29]. The pseudo-second order model is represented by Eq. (3):

$$Q_t = \frac{k_2 Q_e^2 t}{1 + k_2 Q_e t} \quad (3)$$

where k_2 is associated to the pseudo-second order kinetic adsorption constant ($\text{g mg}^{-1} \text{ min}^{-1}$) [10, 29]. The Elovich model is represented by Eq. (4):

$$Q_t = \frac{\ln(\alpha\beta) + \ln t}{\beta} \tag{4}$$

where α is the initial adsorption rate constant ($\text{mg g}^{-1} \text{ min}^{-1}$) and β is the initial desorption rate constant (g mg^{-1}) [10, 29].

2.7 Isotherms

The adsorption isotherms were performed for AL:PVA membranes to obtain information on the adsorption sites and the type of reaction occurring. For these tests, 50 ppm solutions of FLX were prepared as typical adsorption tests. Samples were collected at 0 and 180 min (equilibrium). From those samples, the concentration (C_e) and adsorption capacity (Q_e) at equilibrium were calculated. Isotherms are obtained by varying the mass of adsorbents (resulting in a varying adsorption capacity and concentration at equilibrium) at fixed temperatures. For our tests, adsorbent masses of 5, 10, 15, 20, 25, 30 and 35 mg were tested and temperatures of 25, 40 and 60°C were compared. The curves obtained by plotting the C_e versus Q_e are then compared to isotherm models (Freundlich, Langmuir, Sips, Redlich-Peterson) to gain important information. **Table 1** shows the different equations for the models studied.

Here, Q_e is the adsorption capacity at equilibrium (mg/g), C_e is the concentration in solution at equilibrium (ppm), k_F is the Freundlich isotherm constant ($\text{mg/g [L/mg]}^{1/n}$), n is the heterogeneity factor (dimensionless), Q_{max} is the maximum adsorption capacity (mg/g), k_L is the Langmuir isotherm constant (L/mg), k_S is the Sips isotherm constant ($[\text{L/mg}]^{1/n}$), k_R is the Redlich-Peterson isotherm constant (L/g), a_R being the Redlich-Peterson isotherm constant ($[\text{L/g}]^{b_R}$) and b_R is the Redlich-Peterson model exponent (dimensionless).

2.8 Thermodynamic study

The thermodynamic parameters (enthalpy, entropy and Gibbs’s free energy) are calculated through a thermodynamic study. These parameters are obtained by using the C_e and Q_e recovered from isotherms adsorption tests and the Van’t Hoff and 2nd thermodynamic law equations. The Van’t Hoff equation corresponds to:

$$\ln \frac{Q_e}{C_e} * 1000 \frac{\text{g}}{\text{L}} = \frac{\Delta S^\circ}{R} - \frac{\Delta H^\circ}{RT} \tag{5}$$

Models	Non-linear equation	Equation
Freundlich	$Q_e = k_F C_e^{1/n}$	(5)
Langmuir	$Q_e = \frac{Q_{max} k_L C_e}{1 + k_L C_e}$	(6)
Sips	$Q_e = \frac{Q_{max} k_S C_e^{1/n}}{1 + k_S C_e^{1/n}}$	(7)
Redlich-Peterson	$Q_e = \frac{k_R C_e}{1 + a_R C_e^{b_R}}$	(8)

Table 1.
Isotherm models non-linear equations [10, 30].

where ΔS° is the standard entropy ($\text{J mol}^{-1} \text{K}^{-1}$) and ΔH° is the standard enthalpy (J mol^{-1}) [31]. The second thermodynamic law equation corresponds to:

$$\Delta G^\circ = \Delta H^\circ - T\Delta S^\circ \quad (6)$$

where ΔG° is the standard Gibbs's free energy (J mol^{-1}) [31]. These values will give information on the amount of thermal energy produced, the energy of the bonds, the spontaneity of the reaction and the favourability of an adsorption reaction.

2.9 Desorption tests

The capacity of an adsorbent to be desorbed is also an important characteristic value since it can have a significant contribution on economics and life cycle assessment of the process. Therefore, the reusability of the AL:PVA membranes was evaluated by desorption. For this purpose, multiple conditions were tested to recover the contaminant safely. Hence, the nanofibres were exposed to solutions of methanol (to create an environment in which the contaminant is highly soluble), purified water (to verify the risk of desorption due to equilibrium), heated solutions (might be able to revert the sorption reaction), salts (ion exchange and/or competition) and combined techniques (except heated methanol solutions). In all cases, the membranes were immersed in 50 mL of solution for 4 h. For temperature effect, solutions were heated to 60°C to verify desorption. The salt used for desorption was sodium chloride since it is a simple and non-toxic substance, largely found in typical wastewater. Concentrations of sodium chloride of 1, 2 and 3 M were tested. Initial and final samples were injected in HPLC-DAD to determine the concentration of FLX recovered. The desorption solution showing the best desorption efficiency was used for repeated adsorption/desorption cycles to evaluate the reusability. Between each test, the membranes were recovered and dried in a vacuum desiccator to prevent humidity from interfering with the measured masses. For membranes exposed to salts, these were washed several times with purified water to dissolve salts, and then dried in a vacuum desiccator.

3. Results and discussion

3.1 Electrospinning and nanofibre stabilization

Mixed solutions of AL and PVA were prepared for the production of membranes for adsorption tests. Using the specified electrospinning parameters, it was possible to obtain steady nanofibre formation for periods of a few hours to produce thin nanofibrous mats. Those were thermally stabilized giving the nanofibres a brownish colour and more rigidity. Their immersion in a sodium citrate buffer finalized the stabilization process to provide fibres stability at various pHs enabling their use for adsorption. As shown in **Figure 2**, the stabilization process had a slight impact on the visual aspects of the membranes. However, the impact is more obvious when seen by scanning electron microscopy. **Figure 2b** shows that nanofibres of 183 ± 5 nm in diameter were obtained by the electrospinning with a low number of beads or defects. This size does not technically correspond to nanofibres (0–100 nm), but the adsorption properties shall be akin to real nanofibres considering the small difference. **Figure 2d** shows the nanofibres after a thermal process. This image shows a similar nanofibrous aspect with small variations of the nanofibre diameter (156 ± 5 nm). However, nanofibres seem to be closer to each other with slight cross-linking giving it

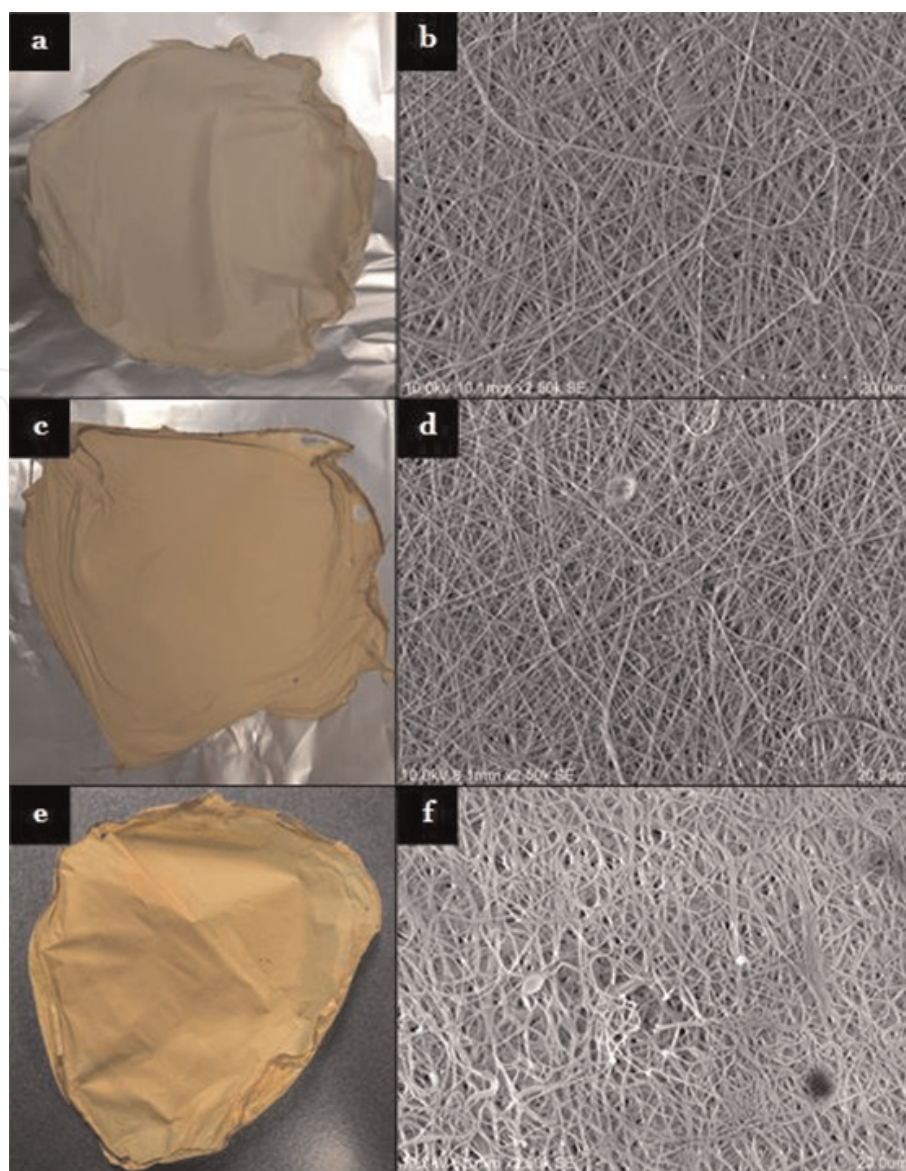


Figure 2.

Images of AL:PVA nanofibres after electrospinning (a), after thermal treatment (c) and after final chemical treatment (e) and corresponding MEB images at 2500× (b, d and f, respectively).

rigidity. With the chemical stabilization (**Figure 2f**), the cross-linking is obvious due to swelling and fusing of nanofibres (188 ± 10 nm). However, it should be emphasized that this kind of treatment often causes the loss of porosity of the material. In fact, without the thermal process, the acid treatment causes the nanofibres to completely fuse together lowering the porosity of the material [26, 32].

Interestingly, humidity had a real impact on the different steps of electrospinning. In fact, at low humidity (e.g., 10%), it was possible to electrospin, but the efficiency was lower. This might be due to the fast evaporation of the solvent during electrospinning which caused the drop of polymers at the tip of the needle to dry before electrospinning or the electrospinning jet to break before reaching the collector surface. The recovery of nanofibres was also more difficult due to higher adherence to the metal plates. At higher humidity (between 30 and 40%), the electrospinning resulted in a larger nanofibre mat surface area on the collector, which was easily peeled off, almost without the use of a razor blade. The advantages of the higher humidity also appeared during the stabilization step. Indeed, a higher humidity reduced the drying speed of the membranes, but also reduced their stickiness to the collector plate. It is therefore important to control the humidity within a certain range to achieve good nanofibre mat formation and easy processability.

3.2 General adsorption

The adsorption tests were first conducted for FLX since it has the most potential for adsorption. Therefore, 25mg of AL:PVA nanofibres were used to adsorb 50 ppm of FLX in a 50 mL solution. The test lasted 150 min with a sample collected at the beginning and at the end. **Table 2** shows the results obtained for this adsorption test. For comparison purposes of the adsorption, the same test was also carried out using commercial adsorbents. However, considering the smaller size of the commercial adsorbent, adjustments were necessary to conduct adsorption tests without any bias. Hence, the volume of the solution was reduced to 10 mL and the concentration was risen to 250 ppm to keep the same mass of FLX (2.5 mg solution) for the same mass of adsorbents. Therefore, the maximum adsorption capacity obtainable for each test was 100 mg/g. The summary of these results is available in **Table 2**.

As expected, unfunctionalized silica adsorbents (Siliaflash[®] and fumed silica) had low adsorption potential for FLX. This is due to the lack of functional groups for adsorption and/or ionic charges. Due to its ion-exchange properties, Valfor[®] had a better adsorption propensity than silica. However, considering the exchange mechanism (exchange with a sodium ion from the adsorbent) and the size of the FLX molecules, it is possible that the adsorption was limited by the number of available sites and competition between FLX molecules. This type of sorbent might be more appropriate for metal ions [33]. Both ion-exchange resins had good adsorption capacities. Both being cation exchange resins and strongly acidic, they possessed functional groups (sulfate) appropriate for the adsorption of ionic molecules such as alkaline pharmaceutical residues. It is therefore encouraging that a biosorbent made of lignin can yield similar or better adsorption capacities than commercial sorbents.

For a potential application in wastewater treatments, it is important to evaluate its capacity to adsorb multiple and various contaminants at the same time. Hence, the adsorption capacities of the developed nanofibres were compared with four contaminants, fluoxetine (antidepressant), venlafaxine (antidepressant), carbamazepine (anticonvulsant) and ibuprofen (anti-inflammatory). The adsorption was evaluated separately and simultaneously to detect possible competitions between contaminants (see **Table 3**).

The contaminants having the most affinity for the membranes were in the decreasing order FLX, VEN, CAR and IBU. IBU and CAR had a low affinity for the nanofibres with almost no adsorption in simultaneous adsorption. This follows the logical assumption that could be made from the structures of the molecules and their chemical properties. For instance, both FLX and VEN are alkaline pharmaceuticals that are easily protonated at a neutral pH. However, fluoxetine has more aromatic rings and possesses Fluor promoting hydrogen bonding and π -stacking. For CAR and IBU, the molecules are respectively neutral and anionic at pH 7 which

Adsorbent	Adsorption capacity (mg/g)
AL:PVA nanofibres	78.24 ± 1.35
Amberlyst [®] 15	80.96 ± 0.35
Dowex [®] Marathon [®] C	77.03 ± 0.94
Valfor [®] 100	49.00 ± 4.39
Fumed silica	8.54 ± 0.62
Siliaflash [®] F60	4.25± 0.35

Table 2.
Adsorption capacity comparison of AL:PVA membranes with commercially available adsorbents.

Contaminant	Simultaneous adsorption capacity* (mg/g)	Individual adsorption capacity** (mg/g)
Fluoxetine (FLX)	22.85 ± 0.28	78.24 ± 1.35
Venlafaxine (VEN)	11.05 ± 1.02	49.76 ± 2.80
Carbamazepine (CAR)	1.02 ± 0.02	8.04 ± 0.01
Ibuprofen (IBU)	0.62 ± 0.39	5.00 ± 0.46

*Initial concentration of 12.5 ppm.
**Initial concentration of 50 ppm.

Table 3.
Affinity comparison of the AL:PVA nanofibres for various pharmaceutical contaminants.

completely prevent any ionic bonding between lignin’s phenols and cationic groups from pharmaceuticals. AL is also a weak acid which would hardly make any ionic bonds with an acidic compound such as IBU.

3.3 Kinetic studies

Kinetic studies give interesting data about the reaction order, type and time necessary to reach equilibrium. For this purpose, kinetic curves were plotted by observing the adsorption capacity at multiple times for FLX alone and for the simultaneous adsorption of contaminants. First, adsorption capacity for fluoxetine was measured at 0, 5, 10, 15, 20, 30, 40, 50, 60, 75, 90, 120 and 150 min to obtain a kinetic curve. Using Matlab®, the kinetic models’ parameters were calculated using non-linear regression analysis. These results are shown in **Table 4**. From **Figure 3**, it is possible to observe the different kinetic curves corresponding to pseudo-first and pseudo-second order and Elovich kinetic models as well as the experimental values. From **Figure 3** and **Table 4**, it is clear that the pseudo-first order best fitted the experimental data. The pseudo-first order indicates that the adsorption occurs in one step. Good correlation with this model also shows that the reaction is regulated by the time necessary for the reaction and not by the diffusion in the nanofibrous

Kinetic model	Parameter	Value
Pseudo-first order	R^2	0.9989
	RMSE	0.7117
	K_1 (min ⁻¹)	0.086
	Q_e (mg/g)	63.98
Pseudo-second order	R^2	0.9790
	RMSE	3.046
	K_2 (g/mg/min)	0.0017
	Q_e (mg/g)	71.14
Elovich	R^2	0.9229
	RMSE	5.832
	α (mg/g min)	33.37
	β (g/mg)	0.08453

Table 4.
Kinetic parameters for pseudo-first order, pseudo-second order and Elovich models.

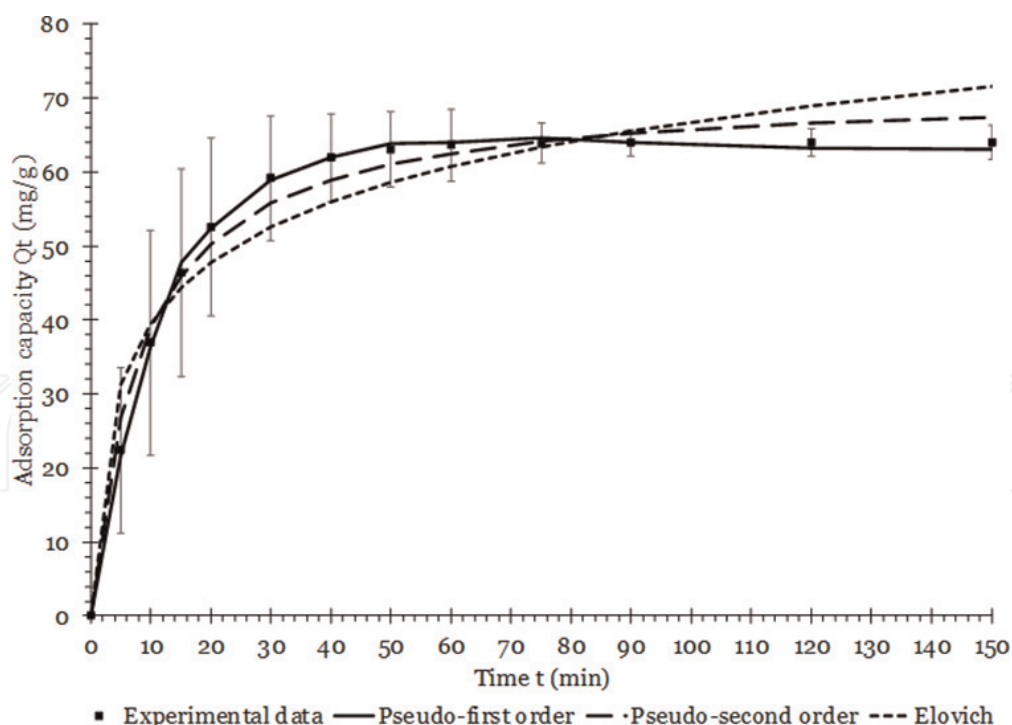


Figure 3.
Kinetic curve for the adsorption of FLX on AL:PVA nanofibres.

material. However, the literature shows that no assumptions can be made from the kinetic model to determine the adsorption mechanism (physisorption or chemisorption for instance) [28]. Still, considering the chemical structure of lignin, physisorption is more logical. For physisorption, the main possible interaction forces are van der Waals, π -stacking, hydrogen bonds, hydrophobicity, steric and polarity interactions [10].

More information can also be obtained from **Figure 3**. For instance, following the observation of the graph, it is possible to conclude that equilibrium is obtained within 1 h and that most of the adsorption occurs in the first 20 min. Such a fast adsorption could allow multiple applications to the adsorbent in addition to the retention of contaminants in wastewater. Also, due to the sampling, the total amount of contaminant available is lower which causes a lower adsorption capacity during kinetics. During the test, it was also possible to follow the adsorption process by monitoring of the pH becoming more acid as the alkaline FLX was removed from the solution.

A kinetic experiment was also conducted with simultaneous contaminants. The kinetic curve for each contaminant is presented in **Figure 4**. For FLX, the curve was almost identical to the individual curve which suggests that no significant competition occurred for FLX. For VEN, the adsorption was significantly longer with equilibrium at 90 min. Its final adsorption capacity, however, remained similar by roughly adsorbing half of the initial concentration. For IBU and CAR, the adsorption was fast (equilibrium within 5 min) and their adsorption capacity was low. Their low adsorption capacities show that AL:PVA membranes might be ineffective for such contaminants except for really low quantities. Coupling AL:PVA nanofibres with other adsorbents could be an alternative to adsorb a wider pharmaceutical contaminants spectrum. For instance, recent studies on chitosan and poly (ethylene oxide) showed good adsorption capacities for IBU in water [32].

3.4 Isotherm studies

The goal of the experiment is to understand the behaviour of adsorption sites while specific changes are made. By monitoring the variation of concentration and

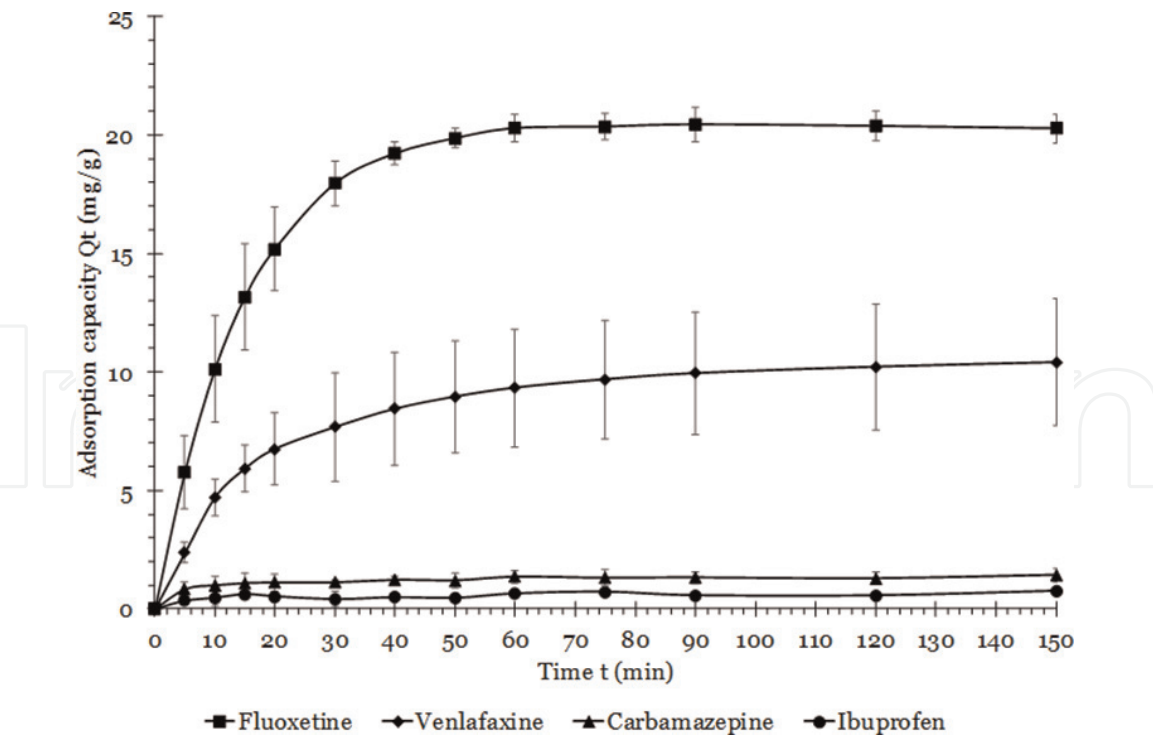


Figure 4.
Kinetic curve for simultaneous adsorption of FLX, VEN, CAR and IBU.

adsorption capacity at equilibrium while varying the mass of adsorbents, it is possible to obtain an isotherm curve which can be compared to isotherm models. The Freundlich, Langmuir, Sips (or Langmuir-Freundlich) and Redlich-Peterson models were compared to the data. The isotherm constants and statistical analysis of the fitting at various temperatures are presented in **Table 5**.

Results show that, for all temperatures, the Sips model best fitted the experimental data with the highest R^2 and RMSE coefficients. This model indicates that a contaminant will link to multiple adsorption sites simultaneously. Also, this model can also be reduced to both Freundlich and Langmuir isotherms depending on the concentration of contaminants (low concentration and high concentration respectively) [10, 27, 30]. Considering that in real remediation conditions the concentrations are lower, it would be appropriate to predict the adsorption to be closer to a Freundlich isotherm. In the Freundlich model, the adsorption occurs in multi-layers with heterogenous sites adsorbing a single molecule [10]. In the Langmuir model, however, the adsorption is in monolayers on homogenous sites [10]. In these types of models, the pH, the temperature and the concentration remain the dominating factors affecting adsorption. This is further observed when the temperature increased and the adsorption capacity accordingly got lower. However, the isotherm models had much lower correlation as the temperature went up.

3.5 Thermodynamic studies

Thermodynamic parameters give interesting information on energy transfers during adsorption. Using the experimental data obtained from fluoxetine's isotherms and Eqs. (9) and (10), standard enthalpy, standard entropy, standard Gibbs's free energy were calculated. For enthalpy, a value of -7987 J/mol or -7.99 kJ/mol was obtained which indicates that the adsorption reaction is exothermic. This means that no heat is necessary for efficient adsorption and that supplying heat would be unfavourable for adsorption in this case. Also, this value falls into the energy

Isotherm	Parameter	25°C	40°C	60°C
Freundlich	R^2	0.9655	0.9510	0.8486
	RMSE	4.716	6.200	6.113
	k_F	11.22	2.298	8.093
	N	0.6441	1.131	0.6326
Langmuir	R^2	0.9783	0.9374	0.8242
	RMSE	3.746	7.006	5.893
	Q_{max}	249.2	3.242e+4	175.3
	k_L	0.02292	1.083e-4	0.02223
Sips	R^2	0.9899	0.9510	0.8877
	RMSE	2.859	6.933	6.079
	Q_{max}	140.3	9.285e+4	82.32
	k_S	0.05902	8.513e-5	0.06166
	N	1.83	1.132	3.277
Redlich-Peterson	R^2	0.9855	0.9510	0.8669
	RMSE	3.423	6.933	6.620
	k_R	4.499	117.5	2.983
	a_R	3.122e-4	50.23	1.523e-4
	b_R	2.021	-0.135	2.183

Table 5.
Isotherm parameters for various isotherm models at 25, 40 and 60°C.

range normally associated with hydrogen bonds (4–50 kJ/mol) and π -stacking (8–12 kJ/mol) [34, 35]. For entropy, a value of 42.01 J/mol. k was obtained. A positive value indicates that there is a gain in entropy and that the reaction is favourable. For ΔG° (at 25°C), a value of -20.51 kJ/mol was calculated which shows that the reaction is spontaneous. Moreover, values close to -20 kJ indicate that physisorption is prevalent [31].

Hence, the adsorption seems to be an appropriate method for water remediation against pharmaceutical contaminants since it consumes low to no energy. Its exothermic nature is also advantageous in cold climate countries like Canada since heating costs would be higher. In addition, it is possible to use the information obtained through thermodynamic to develop a desorption method for nanofibres. For this reason, the use of heated solutions for desorption will be investigated in the next section.

3.6 Desorption and reusability study

One of the benefits of sorption is the possibility of desorption. In this way, multiple adsorption and desorption cycles are possible, and the material is reusable. For these reasons, various desorption solutions were tested on AL:PVA nanofibres for the recovery of FLX. This step's purpose also was obtaining a simpler matrix in which the contaminants can easily be recovered (dried form) or disposed safely. The solutions used had to be either non-toxic or easily evaporated and reused. The effect of temperature was also investigated for a simple desorption method. Results obtained for each tested desorption method are presented in **Table 6**. As shown in this table, the use of an organic solvent such as methanol has the disadvantage of causing

Desorption solution	Fluoxetine recovered (%)	Qualitative result
100% methanol	89	High mass loss
50% methanol	36	Slight mass loss
100% water	1	None
100% water 60°C	30	None
1M NaCl 25°C	52	None
1M NaCl 60°C	92	None
2M NaCl 60°C	76	None
3M NaCl 60°C	19	None

Table 6.
Impact of various desorption solutions on desorption of fluoxetine and AL:PVA nanofibres.

degradation of the membranes in addition to the desorption. Even, it is possible that the desorption detected is due to the degradation of nanofibres. Therefore, pure methanol and 50% methanol solution were discarded. Using pure water, almost no desorption occurred which means that the strength of the bond is sufficiently strong to prevent a new equilibrium. When pure water is heated, however, FLX can be desorbed to some extent (30%) which follows the assumptions made in thermodynamic study. Then, sodium chloride was tested for the desorption of FLX. First, 1 M NaCl solution was tested at room temperature which indicated that salts were effective to recover the pharmaceutical contaminant. Afterwards, the same desorption was tested at 60°C. With this method, more than 90% of the fluoxetine could be recovered without affecting the membrane’s integrity. The concentration of salt was also varied to verify if a higher concentration would give a better desorption. Instead, higher salt concentrations reduced desorption capacity. Considering the difference in size of FLX compared to NaCl, this might be due to the saturation of the solution in which the fluoxetine cannot be dissolved.

To attest the reusability of the membranes, the best desorption method (1M NaCl solution heated to 60°C) was tested for three adsorption/desorption cycles (see **Figure 5**). In this process, the membranes were dried and weighed before each adsorption or desorption tests to observe possible mass loss.

To simplify comparison, **Figure 5** shows the mass of FLX instead of the adsorption capacity. First, it is interesting to observe that the amount desorbed is increasing with desorption cycles. This can be due to a higher number of FLX molecules on the membranes on the second and third cycle (the amount not desorbed on the previous cycles plus the amount adsorbed on the current cycle). Moreover, the adsorption capacity of the membranes was not affected by the desorption as shown by the small rise in mass adsorbed on the third cycle. The small weight gain could have been caused by a slight rise in porosity of the material due to stretching during adsorption and desorption tests. During this test, no significant mass losses were measured through the 3 cycles. Since the membranes are not degrading and do not lose adsorption capacity after the third cycle, it would be logical to assume that the synthesized membranes could still be used for even more cycles.

3.7 Applications and perspectives

The potential of AL:PVA nanofibres was clearly demonstrated through our study. This promising new technology can be exploited in many fields that require adsorption. For instance, the main application dedicated in this study is the adsorption of pharmaceutical contaminants in wastewater. In such application, the

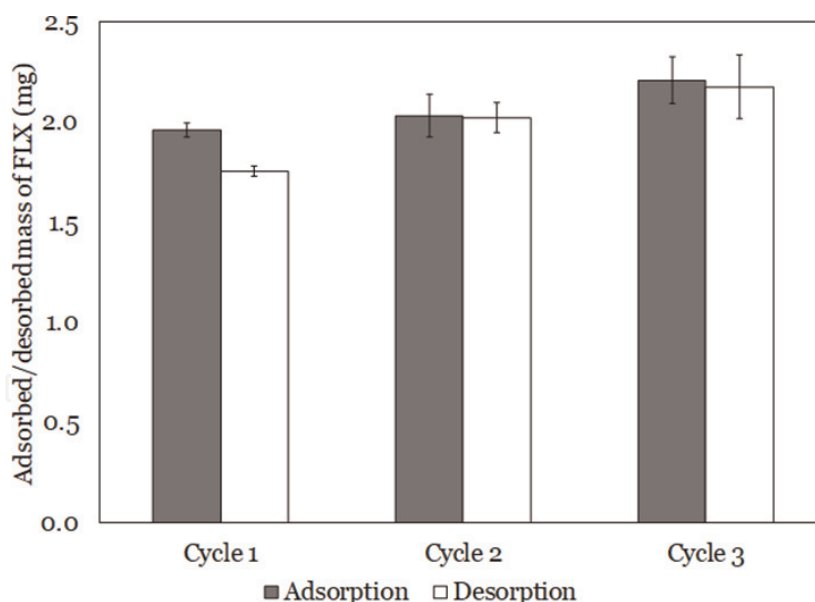


Figure 5.
Adsorption/desorption cycles for FLX using 60°C 1 M NaCl solution.

membranes produced could be incorporated in dynamic systems in wastewater treatment plants or even at the source in hospitals or medical centre effluents. In this way, most of the potentially harmful pharmaceutical residues would be removed and would not enter aquatic ecosystems.

Meanwhile, our research is also investigating the use of nanofibres for the collection and analysis of illicit drugs such as cocaine or methamphetamine. Results obtained from this study will be the object of a future study. However, encouraging results with more than 90% of retention was obtained for both drugs (unpublished results). Moreover, desorption is also efficient. In this way, illicit drugs in complex matrices could be transferred to a simpler matrix for direct analysis in liquid chromatography during forensic investigation.

As of now, the efficiency of the nanofibres was proven for alkaline pharmaceutical contaminants. However, its efficiency is rather poor for contaminants that are neutral or acidic such as CAR or IBU. Therefore, an interesting avenue would be the coupling or sequential use of AL:PVA nanofibres and another biosorbent such as chitosan. In fact, works from our research group showed that chitosan nanofibres are efficient for adsorption of IBU in aqueous medium [32]. Therefore, it would be interesting to test a nanofibrous structure composed of AL and chitosan or a sandwich-like structure made of both types of fibres on mixtures of contaminants. In addition, surface chemical modifications are considered in the near future.

4. Conclusions

Novel alkali lignin and poly (vinyl alcohol) (AL:PVA) nanofibrous membranes were tested for adsorption of pharmaceutical contaminants. Its efficiency to adsorb was first studied on a model contaminant, fluoxetine. An adsorption capacity of 78 mg/g was obtained which corresponds to the adsorption of 78% of fluoxetine present in the water. With further adsorption cycles, the membranes can adsorb up to 90% of contaminants. Compared to commercially available adsorbents (ion-exchange resins, zeolites and silica), the results are similar to costly ion-exchange resins (75–80 mg/g). Using kinetic and isotherm models, it is possible to conclude that nanofibres follow a pseudo-first order kinetic model and Sips' isotherm model

which indicate that the adsorbent is of the physical type with adsorption of the contaminants on multiple sites at the same time in a multi- or monolayer pattern (depending on the concentration). Looking at thermodynamics, adsorption on AL: PVA nanofibres is a favourable, spontaneous and exothermic reaction. This information could be used for the design of a desorption method in which the fluoxetine can be retrieved safely, and the membrane reused for at least two more cycles. The adsorption of multiple pharmaceutical contaminants (fluoxetine, venlafaxine, carbamazepine and ibuprofen) showed that nanofibres have more affinity for alkaline compounds, which adsorb more given the right amount of possible intermolecular forces occurring. Hence, for remediation applications, it would become necessary to combine this adsorbent with another one for maximum retention efficiency.

Acknowledgements

The authors would like to thank the UQTR Foundation, the Innovations Institute for Ecomaterials, Ecoproducts and Ecoenergies Biomass Based, the EcotoQ Research Group and the Forensic Research Group for their financial support during this study. Special thanks are addressed to Agnes Lejeune for her assistance during the collection of SEM images. All technicians at the UQTR are also acknowledged for their technical support.

Conflict of interest

No conflict of interest to declare.

IntechOpen

Author details

Alexandre Camiré¹, Bruno Chabot² and André Lajeunesse^{1,3,4*}

¹ Department of Chemistry, Biochemistry and Physics, Université du Québec à Trois-Rivières, Trois-Rivières, Quebec, Canada


² Innovations Institute in Ecomaterials, Ecoproducts, and Ecoenergies Biomass Based (I2E3), Université du Québec à Trois-Rivières, Trois-Rivières, Quebec, Canada

³ Forensic Research Group, Université du Québec à Trois-Rivières, Trois-Rivières, Quebec, Canada

⁴ EcotoQ Research Group, Institut National de la Recherche Scientifique, Quebec, Canada

*Address all correspondence to: andre.lajeunesse@uqtr.ca

IntechOpen

© 2019 The Author(s). Licensee IntechOpen. This chapter is distributed under the terms of the Creative Commons Attribution License (<http://creativecommons.org/licenses/by/3.0>), which permits unrestricted use, distribution, and reproduction in any medium, provided the original work is properly cited. 

References

- [1] Sousa JCG, Ribeiro AR, Barbosa MO, Pereira MFR, Silva AMT. A review on environmental monitoring of water organic pollutants identified by EU guidelines. *Journal of Hazardous Materials*. 2018;**344**:146-162
- [2] Gavrilescu M, Demnerova K, Aamand J, Agathos S, Fava F. Emerging pollutants in the environment: Present and future challenges in biomonitoring, ecological risks and bioremediation. *New Biotechnology*. 2015;**32**(1):147-156
- [3] Schwarzenbach RP, Egli T, Hofstetter TB, von Gunten U, Wehrli B. Global water pollution and human health. *Annual Review of Environment and Resources*. 2010;**35**(1):109-136
- [4] Oulton RL, Kohn T, Cwiertny DM. Pharmaceuticals and personal care products in effluent matrices: A survey of transformation and removal during wastewater treatment and implications for wastewater management. *Journal of Environmental Monitoring*. 2010;**12**(11):1956-1978
- [5] Cai Z, Dwivedi AD, Lee W-N, Zhao X, Liu W, Sillanpää M, et al. Application of nanotechnologies for removing pharmaceutically active compounds from water: Development and future trends. *Environmental Science: Nano*. 2017;**5**(1):27-47
- [6] Lajeunesse A, Blais M, Barbeau B, Sauvé S, Gagnon C. Ozone oxidation of antidepressants in wastewater-treatment evaluation and characterization of new by-products by LC-QToFMS. *Chemistry Central Journal*. 2013;**7**:15
- [7] Capodaglio AG, Bojanowska-Czajka A, Trojanowicz M. Comparison of different advanced degradation processes for the removal of the pharmaceutical compounds diclofenac and carbamazepine from liquid solutions. *Environmental Science and Pollution Research International*. 2018;**25**(28):27704-27723
- [8] Yin L, Wang B, Yuan H, Deng S, Huang J, Wang Y, et al. Pay special attention to the transformation products of PPCPs in environment. *Emerging Contaminants*. 2017;**3**(2):69-75
- [9] Calisto V, Ferreira CI, Oliveira JA, Otero M, Esteves VI. Adsorptive removal of pharmaceuticals from water by commercial and waste-based carbons. *Journal of Environmental Management*. 2015;**152**:83-90
- [10] Mansour F, Al-Hindi M, Yahfoufi R, Ayoub GM, Ahmad MN. The use of activated carbon for the removal of pharmaceuticals from aqueous solutions: A review. *Reviews in Environmental Science and Bio/Technology*. 2017;**17**(1):109-145
- [11] Sarma H, Lee W-Y. Bacteria enhanced lignocellulosic activated carbon for biofiltration of bisphenols in water. *Environmental Science and Pollution Research*. 2018;**25**(18):17227-17239
- [12] Wertz J-L, Richel A, Gérin P. Molecules derived from valorization of lignin. Contract No.: March. 2015
- [13] Norgren M, Edlund H. Lignin: Recent advances and emerging applications. *Current Opinion in Colloid and Interface Science*. 2014;**19**(5):409-416
- [14] Yang Q, Pan X. Correlation between lignin physicochemical properties and inhibition to enzymatic hydrolysis of cellulose. *Biotechnology and Bioengineering*. 2016;**113**(6):1213-1224
- [15] Zhu W, Theliander H. Precipitation of lignin from softwood black liquor: An investigation of the equilibrium and

molecular properties of lignin.

BioResources. 2015;**10**(1):1696-1714

[16] Wysokowski M, Klapiszewski L, Moszynski D, Bartczak P, Szatkowski T, Majchrzak I, et al. Modification of chitin with Kraft lignin and development of new biosorbents for removal of cadmium(II) and nickel(II) ions. *Marine Drugs*. 2014;**12**(4):2245-2268

[17] Berrima B, Maatar W, Mortha G, Boufi S, El Aloui L, Belgacem M. Adsorption of heavy metals on charcoal from lignin. *Cellulose Chemistry and Technology*. 2016;**50**:701-709

[18] Šćiban MB, Klačnja MT, Antov MG. Study of the biosorption of different heavy metal ions onto Kraft lignin. *Ecological Engineering*. 2011;**37**(12): 2092-2095

[19] Nair V, Panigrahy A, Vinu R. Development of novel chitosan–lignin composites for adsorption of dyes and metal ions from wastewater. *Chemical Engineering Journal*. 2014;**254**:491-502

[20] Ortiz JE, Chabot B. Electrospun nanofibers for the removal of heavy metals from aqueous solutions. Mitacs Globalink Internship Report. Monterrey, Mexico: Monterrey Institute of Technology and Higher Education; July 2016

[21] Chang C-Y, Chang F-C. Development of electrospun lignin-based fibrous materials for filtration applications. *BioResources*. 2016;**11**(1): 2202-2213

[22] Aslanzadeh S, Zhu Z, Luo Q, Ahvazi B, Boluk Y, Ayranci C. Electrospinning of colloidal lignin in poly(ethylene oxide)/N,N-dimethylformamide solutions. *Macromolecular Materials and Engineering*. 2016;**301**(4):401-413

[23] Fang W, Yang S, Yuan T-Q, Charlton A, Sun R-C. Effects of various

surfactants on alkali lignin

electrospinning ability and spun fibers. *Industrial and Engineering Chemistry Research*. 2017;**56**(34):9551-9559

[24] Beck RJ, Zhao Y, Fong H, Menkhaus TJ. Electrospun lignin carbon nanofiber membranes with large pores for highly efficient adsorptive water treatment applications. *Journal of Water Process Engineering*. 2017;**16**:240-248

[25] Fang W, Yang S, Wang X-L, Yuan T-Q, Sun R-C. Manufacture and application of lignin-based carbon fibers (LCFs) and lignin-based carbon nanofibers (LCNFs). *Green Chemistry*. 2017;**19**(8):1794-1827

[26] Camire A, Espinasse J, Chabot B, Lajeunesse A. Development of electrospun lignin nanofibers for the adsorption of pharmaceutical contaminants in wastewater. *Environmental Science and Pollution Research International*. 2018:1-14

[27] Worch E. *Adsorption Technology in Water Treatment: Fundamentals, Processes, and Modeling*. Berlin: De Gruyter; 2012

[28] Tan KL, Hameed BH. Insight into the adsorption kinetics models for the removal of contaminants from aqueous solutions. *Journal of the Taiwan Institute of Chemical Engineers*. 2017; **74**:25-48

[29] Largitte L, Pasquier R. A review of the kinetics adsorption models and their application to the adsorption of lead by an activated carbon. *Chemical Engineering Research and Design*. 2016; **109**:495-504

[30] Foo KY, Hameed BH. Insights into the modeling of adsorption isotherm systems. *Chemical Engineering Journal*. 2010;**156**(1):2-10

[31] Anastopoulos I, Kyzas GZ. Are the thermodynamic parameters correctly

estimated in liquid-phase adsorption phenomena? *Journal of Molecular Liquids*. 2016;**218**:174-185

[32] Paradis-Tanguay L, Camiré A, Renaud M, Chabot B, Lajeunesse A. Sorption capacities of chitosan/polyethylene oxide (PEO) electrospun nanofibers used to remove ibuprofen in water. *Journal of Polymer Engineering*. 2019;**39**(3):207-215

[33] Dragan ES, Dinu M, Shankar G. Recent developments in composite biosorbents and their applications for wastewater treatment. *Research Journal of Chemistry and Environment*. 2015;**19**(11):42-58

[34] Riley KE, Ford CL, Demouchet K. Comparison of hydrogen bonds, halogen bonds, $C H \cdots \pi$ interactions, and $C X \cdots \pi$ interactions using high-level ab initio methods. *Chemical Physics Letters*. 2015;**621**:165-170

[35] Wendler K, Thar J, Zahn S, Kirchner B. Estimating the hydrogen bond energy. *The Journal of Physical Chemistry A*. 2010;**114**(35):9529-9536